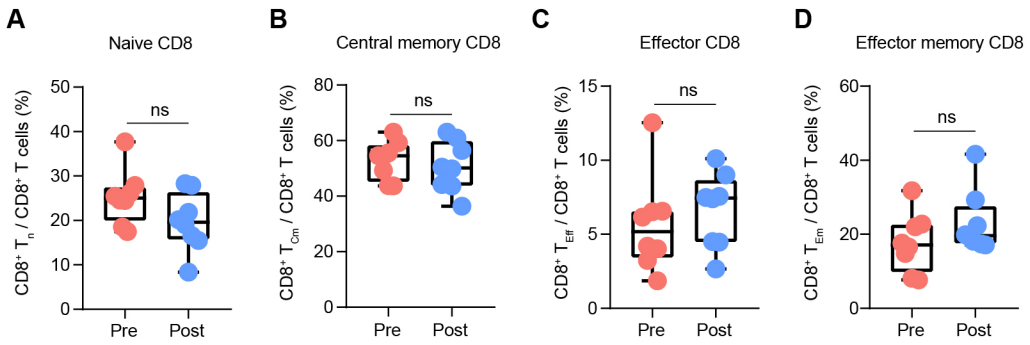

Figure S1. The effects of IFN-α in combination with an anti-PD-1 antibody on HCC patients' peripheral subpopulations of CD8⁺ T cells.

(A-D) Percentages of subpopulations of CD8⁺ T cells in the peripheral blood collected from pretreatment versus that collected from post- treatment of PD-1 blockade and IFN-α (n=8). All data presented are shown as the mean ± SD.

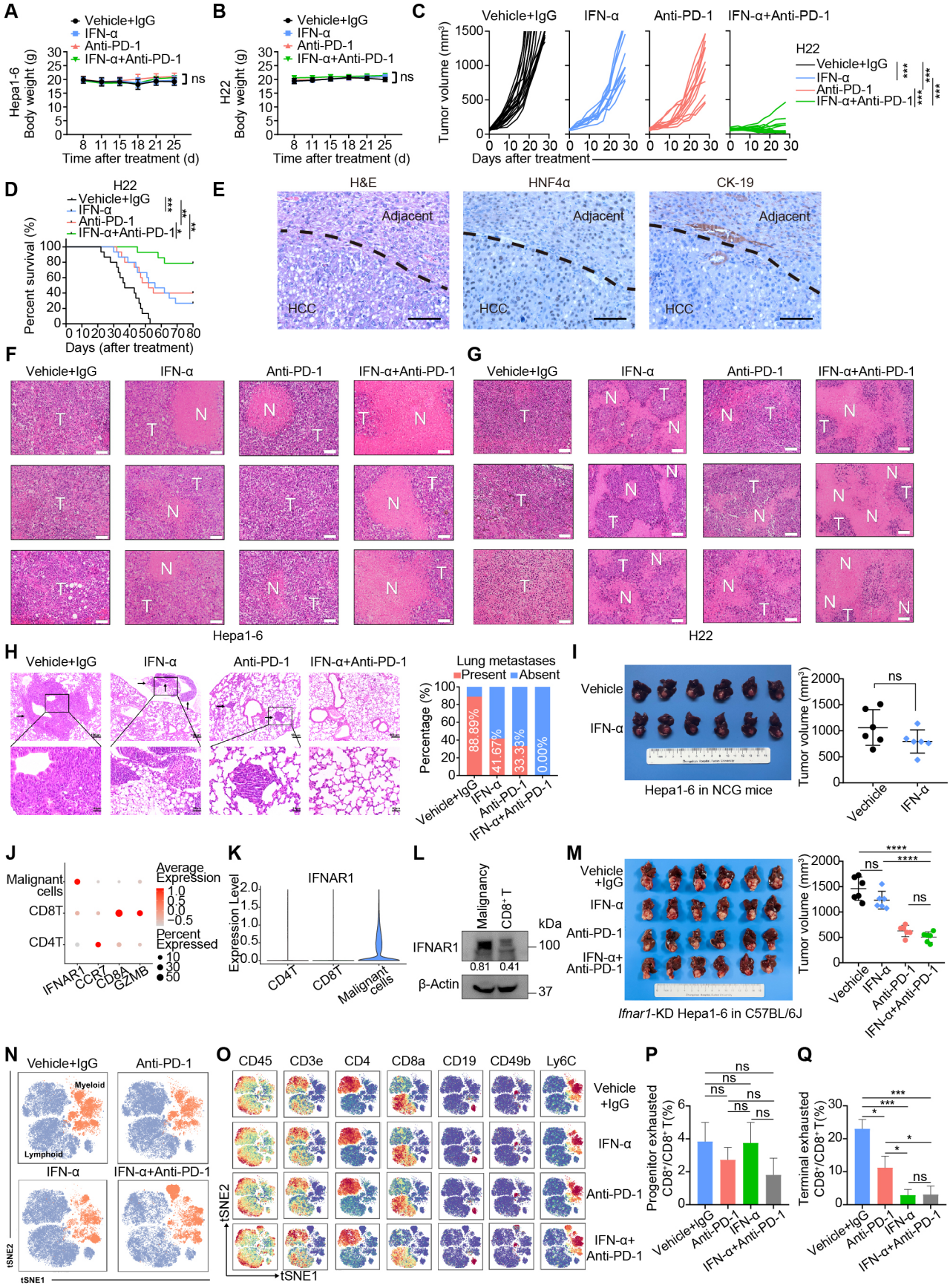
A
Vehicle+IgG
IFN-α
Anti-PD-1
IFN-α+Anti-PD-1
Hepa1-6
Body weight (g)
ns
Time after treatment (d)
B
H22
C
Tumor volume (mm³)
Days after treatment
D
Percent survival (%)
Days (after treatment)
E
H&E
HNF4α
CK-19
Adjacent
HCC
F
Hepa1-6
G
H22
H
Lung metastases
Present
Absent
Percentage (%)
88.89%
41.67%
33.33%
0.00%
I
Vehicle
IFN-α
Hepa1-6 in NCG mice
Vechicle
J
Malignant cells
CD8T
CD4T
Average Expression
Percent Expressed
IFNAR1
CCR7
CD8A
GZMB
K
IFNAR1
Expression Level
CD4T
CD8T
Malignant cells
L
Malignancy
CD8⁺ T
kDa
IFNAR1
β-Actin
0.81
0.41
M
Vehicle +IgG
Anti-PD-1
IFN-α+ Anti-PD-1
Ifnar1-KD Hepa1-6 in C57BL/6J
N
Myeloid
Lymphoid
tSNE1
tSNE2
O
CD45
CD3e
CD4
CD8a
CD19
CD49b
Ly6C
P
Progenitor exhausted CD8⁺/CD8⁺T(%)
Q
Terminal exhausted CD8⁺/CD8⁺T(%)

Figure S2. IFN-α in combination with an anti-PD-1 antibody augmented antitumor immunity and altered the immune landscape of the TME.

(A-B) Body weight of Hepa1-6 **(A)** and H22 **(B)** tumor-bearing mice treated with vehicle + 10 mg/kg IgG, 1 x 10^4 IU IFN-α, 10 mg/kg anti-PD-1, or the combination therapy.

(C) Growth curves of H22 tumors in BALB/c mice (vehicle + IgG, 10 mg/kg, n = 18; IFN-α, 1 x 10^4IU, n = 12; anti-PD-1, 10 mg/kg, n = 12; combination therapy, n = 15).

(D) Survival curves of BALB/c mice bearing H22 tumors (n=15 per group) who received 10 mg/kg IgG, 1 x 10^4 IU IFN-α, 10 mg/kg anti-PD-1, or the combination therapy.

(E) HNF4α and CK-19 immunohistochemistry on liver sections obtained from spontaneous HCC model. Nuclear staining indicated HNF-4α positive cells in the middle panel. Scale bars: 100 μm.

(F-G) Representative hematoxylin-eosin staining of Hepa1-6 **(F)** and H22 **(G)** tumor tissues in the indicated groups. T, tumor; N, necrotic region.

(H) Representative hematoxylin-eosin staining of lungs from mice bearing H22 tumors (vehicle + IgG, 10 mg/kg, n = 18; IFN-α, 1 x 10^4IU, n = 12; anti-PD-1, 10 mg/kg, n = 12; combination therapy, n = 15) and the incidence of lung metastasis in the indicated groups.

(I) At the indicated end points, Hepa1-6 tumor-bearing NCG mice treated with vehicle or 1 x 10^4 IU IFN-α were sacrificed, and the livers from the mice are shown.

(J) Expression pattern of indicated genes among malignant cells, $CD8^+$ T, and $CD4^+$ T cells according to single-cell sequencing data of a previous report[29].

(K) Expression levels of *IFNAR1* among malignant cells, $CD8^+$ T, and $CD4^+$ T cells according to published single-cell sequencing data.

(L) Immunoblotting assay results for IFNAR1 between malignant and $CD8^+$ T derived from orthotopic Hepa1-6 mice models.

(M) *Ifnar1* expression was silenced by using shRNA, and *Ifnar1*-knocked down Hepa1-6 cells were transplanted to generate orthotopic mice models, followed by indicated treatment. The livers bearing Hepa1-6 tumors after distinct treatment were shown (left). Quantifications of volume of *Ifnar1*-knocked down tumors after receiving indicated treatment (right).

(N) t-SNE plots of infiltrating lymphoid compartment (blue) and myeloid compartment (orange) by CyTOF analysis from Hepa1-6 tumors given the indicated treatment.

(O) t-SNE plots of infiltrating immune cells colored by the relative expression of the indicated markers in each group.

(P) Proportions of progenitor exhausted $CD8^+$ T cells in tumor tissues derived from murine models received indicated therapy were analyzed by flow cytometry assays.

(Q) Proportions of terminal exhausted $CD8^+$ T cells in tumor tissues derived from murine models received indicated therapy were analyzed by flow cytometry assays.

The results are shown as the mean ± SD and the statistical significance of differences between groups was determined by an unpaired Student's *t* test.

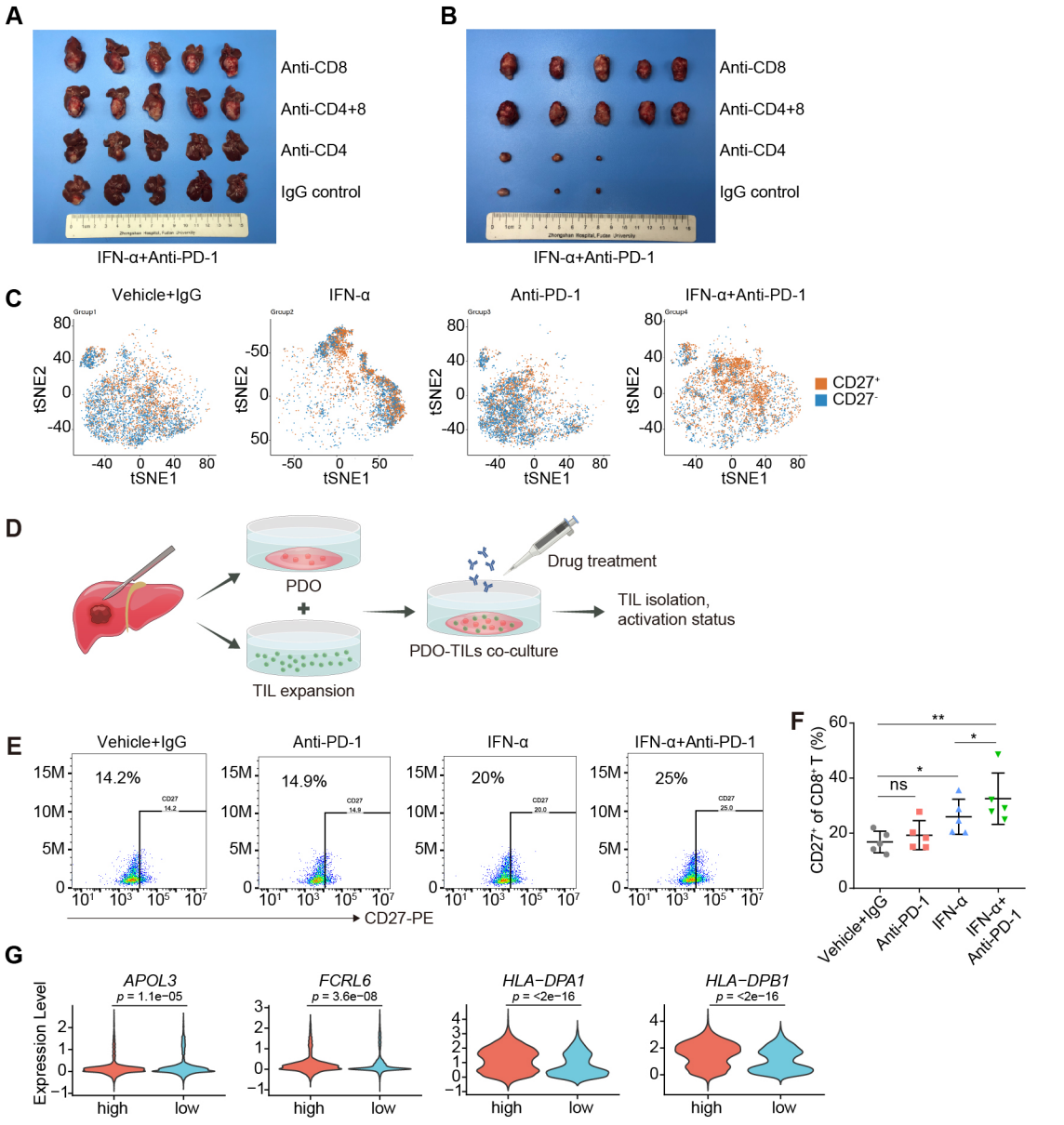

Figure S3. IFN-α plus an anti-PD-1 antibody exerted antitumor effects in a CD8⁺ T cell-dependent manner, and CD27⁺ CD8⁺ T cells correlated with immune activation.

(A-B) At the indicated end points, mice treated with 10 mg/kg IgG, 10 mg/kg anti-CD4, 10 mg/kg anti-CD8, or both depleting antibodies were sacrificed. The livers bearing Hepa1-6 tumors **(A)** and the related Hepa1-6 tumors **(B)** are shown.

(C) t-SNE plots showing the relative expression of CD27 in CD8⁺ T cells for each treatment condition.

(D) A graph abstract of HCC patient-derived organoid and autologous intratumoral immune cells co-culture model.

(E-F) Tumor cells and CD8⁺ tumor infiltrating lymphocytes (TILs) were isolated from same HCC patient (n=5) and cultured respectively for 3 days. On day 3, HCC organoids and CD8⁺TILs were directly co-cultured in 5:1 ratio, supplemented with 1 x 10^4 IU/ml IFN-α plus 100 μg/ml anti-PD-1 antibody. After 72 hours of co-culture, the CD27⁺CD8⁺ T cell population was evaluated by flow cytometry.

(G) Violin plot showing *CD27* expression in the indicated clusters from HCC patients evaluated by single-cell sequencing.

The results are shown as the mean ± SD for experiments performed in triplicate. Each experiment was repeated three times, and the statistical significance of differences between groups was determined by an unpaired Student's *t* test.

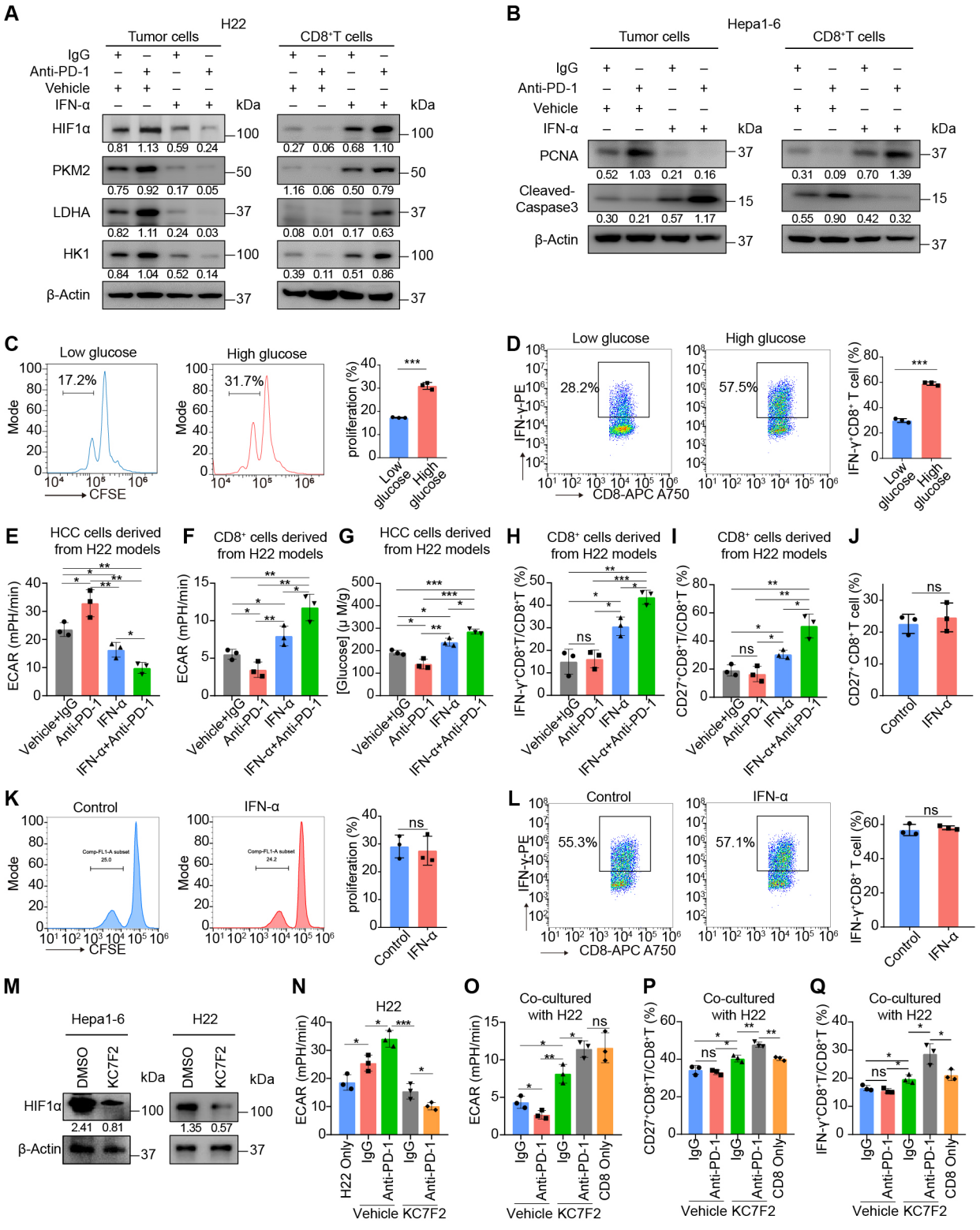

Figure S4. IFN-α hindered glycolysis in tumors by inhibiting HIF1α signaling to foster the activation of CD8⁺ T cells.

(A) Immunoblot assays for HIF1α, PKM2, LDHA, and HK1 in H22 cells and CD8⁺ T cells derived from distinct mouse models that received the indicated treatments. IFN-α concentration: 1 x 10^4 IU; anti-PD-1 concentration: 10 mg/kg. β-Actin was used as an internal control.

(B) PCNA and cleaved Caspase-3 expression in HCC and $CD8^+$ T cells derived from Hepa1-6 mouse models that received the indicated treatments was determined by immunoblot assays. IFN-α concentration: 1 x 10^4 IU; anti-PD-1 concentration: 10 mg/kg. β-Actin was used as an internal control.

(C) CFSE-labeled murine spleen $CD8^+$T cells were cultured in the present of αCD3 and αCD28 in low-glucose (5 mM) or high-glucose (25 mM) RPMI medium, respectively, for three days. The fluorescence of CSFE was measured by flow cytometry. The proliferation rate of T cells was determined as the proportion of cells with reduced CFSE intensity due to cell division.

(D) Murine spleen $CD8^+$T cells were cultured in the present of αCD3 and αCD28 in low-glucose (5 mM) or high-glucose (25 mM) RPMI medium, respectively, for three days. IFN-γ^+CD8^+T cells were gated and calculated.

(E) ECAR results for tumor cells derived from distinct H22 mouse models that received IgG, 10 mg/kg anti-PD-1, 1 x 10^4 IU IFN-α or combination treatment.

(F) ECAR results for $CD8^+$ T cells derived from different H22 mouse models that received IgG, 10 mg/kg anti-PD-1, 1 x 10^4 IU IFN-α or combination treatment.

(G) Glucose concentration in the extracellular milieu of HCC tissues derived from different H22 mouse models that received IgG, 10 mg/kg anti-PD-1, 1 x 10^4 IU IFN-α or combination treatment.

(H) IFN-γ^+ $CD8^+$ T cells derived from different H22 mouse models that received IgG, 10 mg/kg anti-PD-1, 1 x 10^4 IU IFN-α or combination treatment.

(I) $CD27^+$ $CD8^+$ T cells derived from different H22 mouse models that received IgG, 10 mg/kg anti-PD-1, 1 x 10^4 IU IFN-α or combination treatment.

(J) Murine spleen $CD8^+$T cells were activated in the present of αCD3 and αCD28 for three days and then treated with or without IFN-α for another 24 hours. $CD27^+CD8^+$ T cells were measured by flow cytometry.

(K) CFSE-labeled murine spleen $CD8^+$T cells were activated in the present of αCD3 and αCD28 for three days and then treated with or without IFN-α for another 24 hours. The fluorescence of CSFE was measured by FACS. The proliferation rate of T cells was determined as the proportion of cells with reduced CFSE intensity due to cell division.

(L) Murine spleen $CD8^+$T cells were activated in the present of αCD3 and αCD28 for three days and then treated with or without IFN-α for another 24 hours. For IFN-γ measurement, T cells were stimulated with PMA, ionomycin and golgi block for 4 hours and signals of IFN-γ were determined by flow cytometry.

(M) The efficiency of HIF1α inhibition (10 μM KC7F2) in Hepa1-6 (left) and H22 (right) cells was validated by immunoblot assay.

(N) ECAR results for H22 cells that received IgG or 100 μg/ml anti-PD1 treatment with or without 10 μM KC7F2.

(O) ECAR results for $CD8^+$ T cells after coculture with H22 cells that received IgG or 100 μg/ml anti-PD-1 treatment with or without 10 μM KC7F2.

(P) $CD27^+$ proportion of $CD8^+$ T cells after coculture with tumor cells that received IgG or 100 μg/ml anti-PD1 treatment with or without 10 μM KC7F2.

(Q) IFN-γ^+ proportion of $CD8^+$ T cells after coculture with tumor cells that received IgG or 100 μg/ml anti-PD1 treatment with or without 10 μM KC7F2.

The results are shown as the mean ± SD for experiments performed in triplicate. Each experiment was repeated three times, and the statistical significance of differences between groups was determined by an unpaired Student's *t* test.

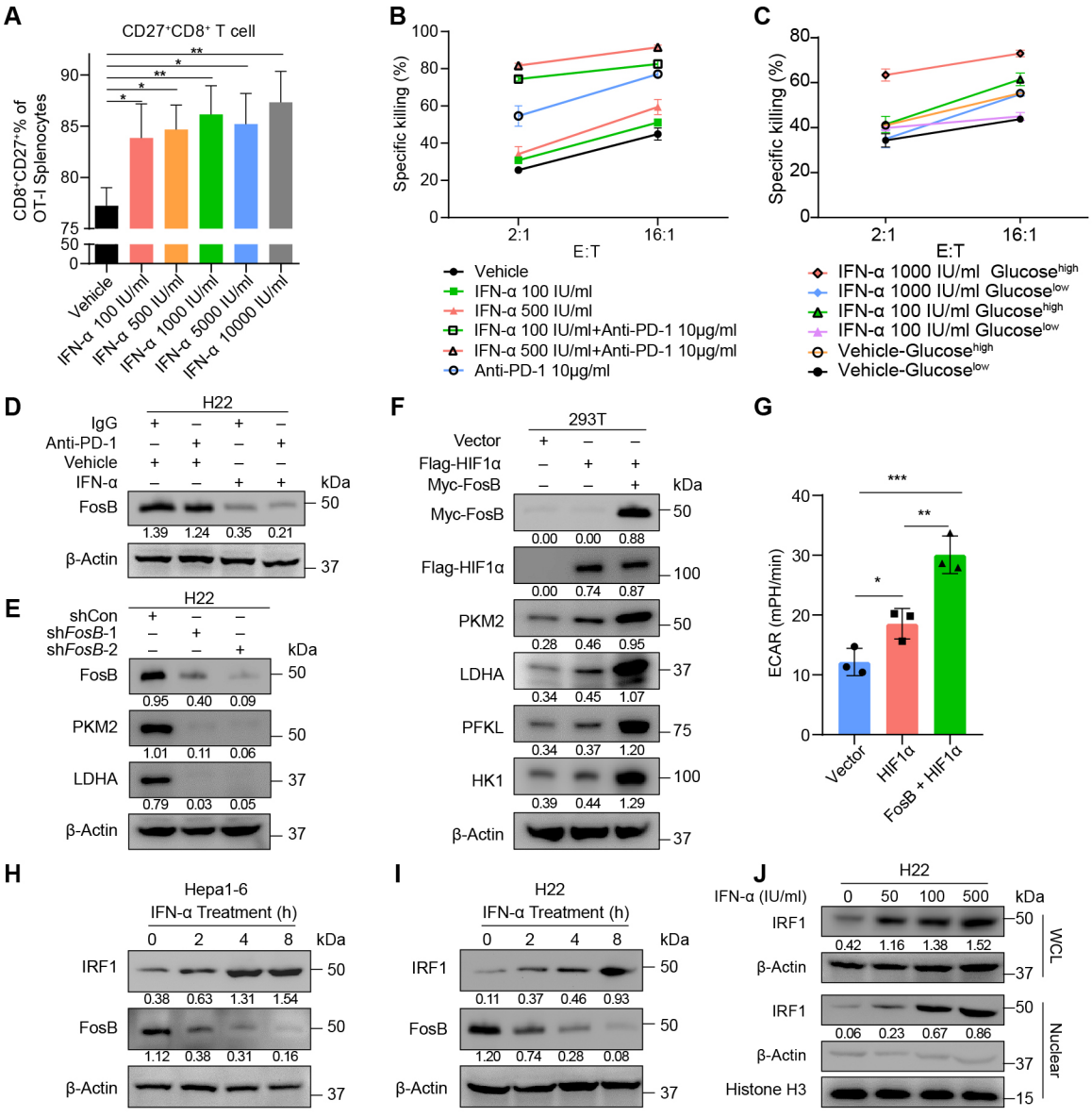

Figure S5. IFN-α treatment restricted HIF1α signaling by restraining the expression of FosB, a cotranscriptional effector of HIF1α, in an IRF1-dependent manner.

(A) After 48 h of IFN-α treatment, CD27 expression in OT-I CTLs which co-cultured with EL4 cells was detected by flow cytometry.

(B) OT-I mouse cytotoxic T cells were used to detect the activity of the combination of IFN-α and anti-PD-1 *in vitro*. OT-I CTLs were treated with anti-PD-1 antibody and different IFN-α concentrations. Different E:T ratios were used to evaluate activity.

(C) OT-I mouse cytotoxic T cells were used to detect the activity of the combination of IFN-α and distinct concentrations of glucose *in vitro*. OT-I CTLs were treated with low or high glucose and different IFN-α concentrations. Different E:T ratios were used to evaluate activity.

(D) The expression of FosB in tumor cells derived from H22 model mice that received the indicated treatments were detected by immunoblot assays. IFN-α concentration: 1 x 10^4 IU; anti-PD-1 concentration: 10 mg/kg. β-Actin was used as an internal control.

(E) The impacts of *FosB* silencing on PKM2 and LDHA expression in H22 cells were evaluated by immunoblot assays.

(F) HIF1α and FosB were cotransfected into 293T cells, and PKM2, LDHA, PFKL, and HK1 expression was determined by immunoblot assays.

(G) ECAR results for 293T cells transfected with the indicated plasmids.

(H) Impacts of IFN-α exposure duration on FosB expression in Hepa1-6 cells that received 500 IU IFN-α.

(I) Impacts of IFN-α exposure duration on FosB expression in H22 cells that received 500 IU IFN-α.

(J) The impacts of IFN-α on the expression of IRF1 in whole-cell lysates and nuclear fractions of H22 cells were evaluated by nuclear-cytoplasmic fractionation followed by immunoblot assays. IFN-α: 0 IU/ml, 50 IU/ml, 100 IU/ml, or 500 IU/ml.

The results are shown as the mean ± SD for experiments performed in triplicate. Each experiment was repeated three times, and the statistical significance of differences between groups was determined by an unpaired Student's *t* test.

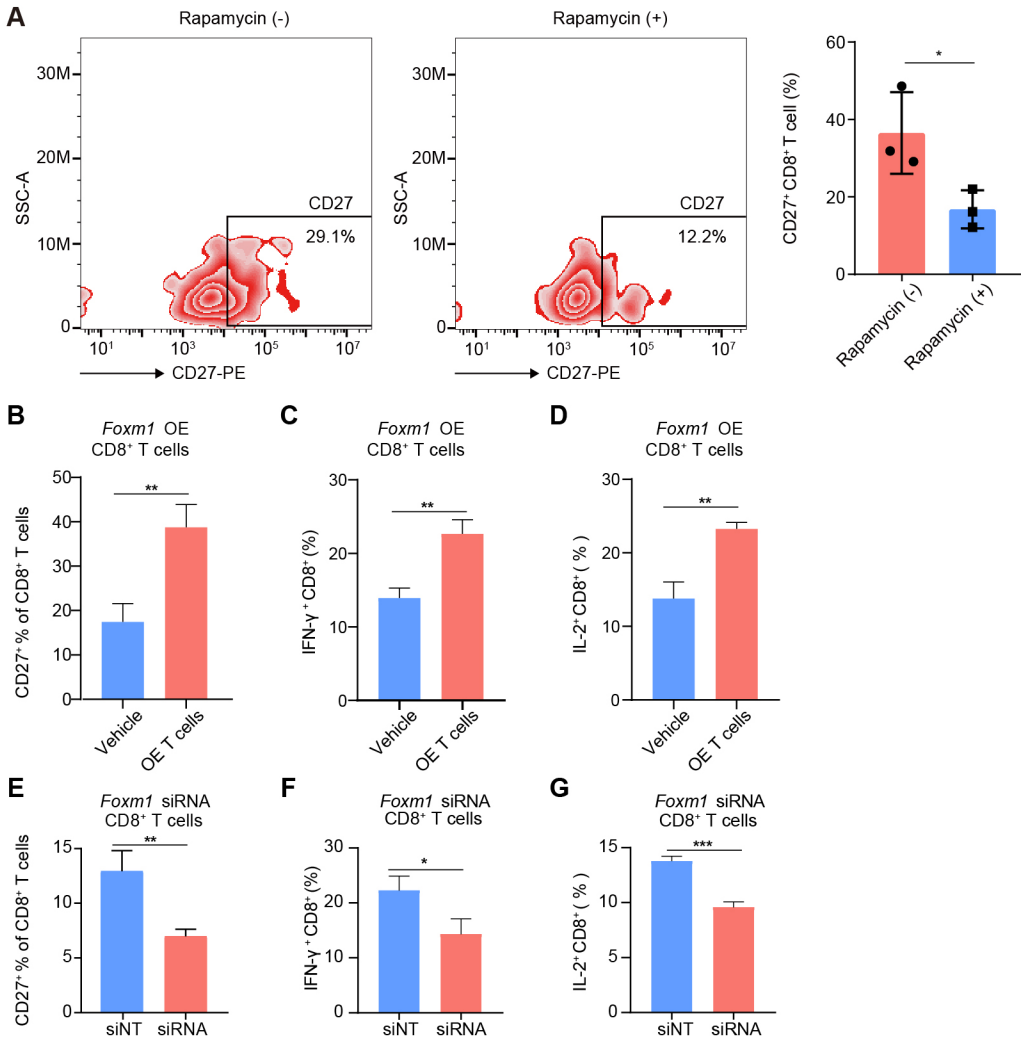

Figure S6. A high-glucose microenvironment promotes CD8⁺ T cell activation via mTOR-induced FOXM1 expression

(A) Paired tumor cells and CD8⁺ tumor infiltrating lymphocytes (TILs) were isolated from HCC patients (n=5) and cultured respectively for 3 days. TILs were pre-treated with or without 200 ng/ml rapamycin for 72 hours. On day 3, HCC organoids and CD8⁺ TILs were directly co-cultured in 5:1 ratio, supplemented with 1 x 10^4 IU/ml IFN-α plus 100 μg/ml anti-PD-1 antibody. After 72 hours of co-culture, the CD27⁺CD8⁺ T cell population was evaluated by flow cytometry. The data are presented as mean ± SD. *$p < 0.05$.

(B) Murine spleen CD8⁺ T cells were isolated and cultured in the presence of αCD3 and αCD28. On the next day, T cells were infected with *Foxm1*-overexpressing or vehicle control retrovirus for another 48 hours. Cells were collected and CD27 signal was measured by flow cytometry.

(C-D) For IFN-γ and IL-2 measurement, T cells were stimulated with PMA, ionomycin and golgi block for 4 hours and signals of IFN-γ **(C)** and IL-2 **(D)** were determined by flow cytometry, respectively.

(E) Murine spleen CD8⁺ T cells were isolated and cultured in the presence of αCD3 and αCD28. On the next day, T cells were transfected with Foxm1-targeting siRNA or control siRNA. 48 hours later, T cells were collected and CD27 signal was measured by flow cytometry.

(F-G) For IFN-γ and IL-2 measurement, T cells were stimulated with PMA, ionomycin and golgi block for 4 hours and signals of IFN-γ **(F)** and IL-2 **(G)** were determined by flow cytometry, respectively.

All data are representative of three independent experiments and presented as mean ± SD. *$p < 0.05$, **$p < 0.01$, ***$p < 0.001$.

Supplementary table 1. Characteristics of the Patients at Baseline.

Characteristics	Patients(N=15)	%
Age at enrollment(years)		
Median(range)	56 (31-69)	
<60 years	10	67
≥60 years	5	33
Sex		
Female	3	20
Male	12	80
Aetiology		
HBV	13	87
HCV	1	7
NASH	0	0
Other	1	7
Tumor size (cm)		
≤5	3	20
>5	12	80
Tumor number		
Single	4	27
multiple	11	73
AFP		
Elevated	10	67
TB		
Elevated	3	20
ALT		
Elevated	4	27
BCLC stage		
A+B	8	53
C+D	7	47
CNLC stage[1]		
I+II	8	53
III+IV	7	47

Abbreviations: AFP, alpha-fetoprotein; ALT, alanine aminotransferase; CNLC stage, China Liver Cancer stage; BCLC stage, Barcelona Clinic Liver Cancer stage.

Reference

1. Zhou J, Sun H, Wang Z, et al. Guidelines for the Diagnosis and Treatment of Hepatocellular Carcinoma (2019 Edition). *Liver Cancer.* 2020;9:682-720.

Supplementary table 2. Antibodies used for CyTOF staining

Isotypes	Antibodies	Clone	Source	Identifier
89Y	CD45	30-F11	BioLegend	103102
115In	CD3e	145.2C11	BioLegend	100302
139La	CD44	IM7	BioLegend	103002
141Pr	CD24	M1/69	BioLegend	101802
142Nd	MHC II	Y3P	Bio-Xcell	BE0178
143Nd	CD45R(B220)	RA3-6B2	BioLegend	103202
144Nd	CX3CR1	SA011F11	BioLegend	149002
145Nd	CD21/CD35	7G6	BD Biosciences	559831
146Nd	IgM	RMM-1	BioLegend	406502
147Sm	CD80	16-10A1	BioLegend	104702
148Nd	Ly-6C	HK1.4	BioLegend	128002
149Nd	CD172a(SIRPα)	P84	BioLegend	144002
150Nd	IgD	11-26c.2a	BioLegend	405702
151Eu	CD62L	MEL14	BioLegend	104402
152Sm	CD11c	N418	BioLegend	117302
153Eu	TCRgd	GL3	in-house	NA
154Sm	Ki-67	SolA15	eBioscience	14-5698-82
155Gd	CD38	90	BioLegend	102702
156Gd	CD317(BST2)	44E9R	R&D systems	MAB8660
157Gd	CD27	LG.3A10	BioLegend	124202
158Gd	CD19	6D5	BioLegend	115502
159Tb	F4/80	C1:A3-1	Bio-RAD	MCA497G
160Gd	CD115(CSF-1R)	AFS98	BioLegend	135502
161Dy	iNOS	CXNFT	eBioscience	14-5920-82
162Dy	CD183(CXCR3)	CXCR3-173	BioLegend	126502
163Dy	CD25	3C7	BioLegend	101902
164Dy	CD103	2E7	BioLegend	121402
165Ho	CD278(ICOS)	C398.4A	BioLegend	313502
166Er	Arginase I	polyclone	Fluidigm	3166023B
167Er	CD49b	DX5	BioLegend	108902
168Er	Foxp3	FJK-16s	eBioscience	14-5773-82
169Tm	CD69	H1.2F3	BioLegend	104502
170Er	CD49a	HMa1	BioLegend	142602
171Yb	CD23	B3B4	BioLegend	101602
172Yb	CD127	A7R34	BioLegend	135002
173Yb	Granzyme B	GB11	Fluidigm	3173006B
174Yb	CD152(CTLA-4)	UC10-4B9	BioLegend	106302
175Lu	TCRab	H57-597	BioLegend	109202
176Yb	CD43	S11	BioLegend	143202
197Au	CD4	RM4-5	BioLegend	100520
198Pt	CD8a	53-6.7	BioLegend	100716
209Bi	CD11b	M1/70	in-house	NA